cal./(mole)(°C). This only slightly raises the value of ΔS_a° to −40.6 cal./(mole)(°C).

The standard enthalpy of adsorption can be converted to the reference state of 1 torr by going through a similar three-step process. Neglecting liquid and gas phase nonideality, one must consider only the enthalpy of vaporization +7.09 kcal./mole (29). Hence, the standard enthalpy change becomes

$$\Delta H_{a,\,1\text{ torr}} = \Delta H_{a,\,\frac{1\text{ mole}}{1\text{ liter}}} - \Delta H_{vap} = -5{,}000 - 7{,}100$$

$$= -12{,}100 \text{ cal./mole}$$

Manuscript received July 22, 1965; revision received September 24, 1965; paper accepted September 27, 1965.

Accessibility of Surface to Gases Diffusing Inside Macroporous Media

W. H. HEDLEY, F. J. LAVACOT, S. L. WANG, and W. P. ARMSTRONG

Washington University, St. Louis, Missouri

A method for measuring flow porosity with values from 35 to 100% of the open porosity measured is described. The accuracy of electrical conductivity measurements to obtain net diffusibilities was verified for media containing at least 75% of pore volume with radii greater than five mean free paths. It is pointed out that long dead-end pores feeding into larger diameter flow pores can contribute to the effective diffusion coefficient inside porous media, and methods of estimating their length and maximum possible contribution to diffusion are described.

The purpose of this work was to develop new techniques of predicting the accessibility of catalyst surface inside macroporous catalysts to diffusing gases. Internal diffusion rates retard many chemical reaction processes that use porous catalysts (*1*), and they can also strongly affect the product composition (*2*). The amount of retardation is expressed by the effectiveness factor, the ratio between the actual rate of a chemical reaction on a heterogeneous catalyst and the rate one would obtain if diffusional effects within the pellet did not retard the reaction. It is a function of a modulus m_T (*3*).

$$m_T = \frac{D_p}{2}\sqrt{\frac{k}{D_{eff}}} \qquad (1)$$

D_p and k can be measured directly, but no methods of measuring D_{eff} which take into account the presence of dead-end pores have been previously described. In this work, a method of estimating limiting values of D_{eff} based on porosity, porosimeter, and either electrical conductivity or gas diffusion measurements is proposed. Once m_T has been calculated from D_{eff}, D_p, and k, the effectiveness factor can be read graphically (*1*).

Wheeler (*2*) pictured porous media as being "piles of boulders between which the continuous, interconnecting pores of irregular cross section run in random direction." Based upon this model, diffusion of two gases in opposite directions *through* a porous medium, herein known as net diffusion, is slower than that which would occur in free space because: diffusion occurs at a noticeable rate only through the pores, not through the solid; some of the pores are dead-end; the pores have constrictions and irregularities in them which retard diffusion; and the pores do not go straight through the medium, increasing the distance that the gases must diffuse. The increased distance for diffusion due to randomness of pore direction has been estimated as being 1.41 times the medium thickness (*2*).

Pores can be classified according to their accessibility. Pore spaces having at least one passage to the exterior are called open pores. Those with only one passage are known as dead-end pores; pores with more than one passage are called flow pores. Only the flow pores are active in electrical conduction (pores filled by conducting liquid) or in simple diffusion of nonreacting gases; how-

W. H. Hedley is with Monsanto Research Corporation, Dayton, Ohio. F. J. Lavacot is with United Aircraft Corporation, Sunnyvale, California. S. L. Wang is with Union Carbide Corporation, Tonawanda, New York.

ever, in a porous catalyst the dead-end pores can also be active, due to inward diffusion of reactant and outward diffusion of product. Thus, a knowledge of the relative proportions of dead-end and flow pores would be helpful for obtaining full understanding and prediction of catalytic performance in macroporous media.

Although methods of measuring open porosity have been available for a long time, methods for measuring flow porosity have been lacking until recently, when Goodknight and Fatt (*4*) suggested one based upon transient flow through porous media, and Stewart et al. (*5*) suggested one based upon sinusoidal flow measurement. Both methods require samples which are considerably larger than the average catalyst pellet.

Schofield and Dakshinamurti (*6*) showed that electrical conductivity measurements made on unconsolidated porous media impregnated with salt solutions could be used to predict the rates of liquid diffusion inside them. Klinkenberg (*7*) postulated that similar measurements could be used to predict the rates of gas diffusion inside porous media. When diffusing gases or electric current are confined inside macropores, the rates of both across porous media should be decreased equally by confinement to open pores, nonconductance of dead-end pores, increased path length due to the wandering of pores in random directions, and constrictions in the irregular cross section of pores. Scott and Cox (*8*) briefly described the results of gas diffusion and electrical conductivity measurements on macroporous media and showed that for the media tested, one could be used to predict the other.

Electrical conductivity measurements are simpler and faster than gas diffusion measurements. Either type will suffice for determining the combined effects of flow porosity, tortuosity, and shape factor, but neither method could measure a contribution of dead-end pores to diffusion in the case of a catalytic chemical reaction.

THEORETICAL

The principal developments in this paper are: the formulation of a method to measure dead-end and flow porosity; verification that electrical conductivity measurements can be used to predict net bulk diffusion of gases inside porous media, provided at least 75% of the pore volume has a diameter greater than five mean free paths; and discussion of cases where dead-end pores, as well as flow pores, can contribute to the effective diffusion coefficient inside a porous medium, thus setting upper and lower limits for this coefficient.

Diffusion

Bulk diffusion occurs in free space and inside pores where the diameter is much greater than the mean free path of the molecules. Bulk diffusion coefficients can be measured either experimentally or be calculated by the methods of Arnold (*9*), Gilliland (*10*), or Hirschfelder, Curtiss, and Bird (*11*). Wheeler suggested that the approximate lower limit for bulk diffusion occurs where the mean free path of the diffusing molecules is ten times the pore radius (*2*). At conditions of one atmosphere absolute pressure and room temperature at which the diffusion measurements in this work were made, Wheeler calculated that bulk diffusion is expected in pores 10^{-4} cm. or larger in radius, Knudsen diffusion in pores with a radius of 10^{-6} cm. or less, and a mixture of the two for pores of intermediate size. Most of the media used in this work had average pore diameters greater than 10^{-4} cm., so that bulk diffusion occurred, although a few had average pore diameters at the upper end of the transition region. Surface diffusion was avoided by using gases at a temperature far above their normal boiling points.

In free space, the equation for steady state counterdiffusion of the gases A and B is written (*12*):

$$\ln\left[\frac{1-\left(1-\frac{N_B}{N_A}\right)\frac{P_{A2}}{P}}{1-\left(1-\frac{N_B}{N_A}\right)\frac{P_{A1}}{P}}\right]=\frac{XRT\,(N_A-N_B)}{D_BP} \tag{2}$$

If this equation is modified for the case of two gaseous components being mixed on either side of a porous medium and counterdiffusing, allowance must be made for the four retarding characteristics mentioned previously and for the thickness of a laminar gas film adjacent to each side of the medium. The four factors are combined into a factor known as net diffusibility δ'.

$$\delta' = (\epsilon_o)\left(\frac{\epsilon_f}{\epsilon_o}\right)(\tau)\ (P_s) \tag{3}$$

which is the ratio of the effective net diffusion coefficient across the porous medium to the diffusion coefficient in free space.

$$D'_{eff} = \delta'\ D_B \tag{4}$$

The equation for counterdiffusion of gases through porous media is

$$\ln\left[\frac{1-\left(1-\frac{N_B}{N_A}\right)\frac{P_{A2}}{P}}{1-\left(1-\frac{N_B}{N_A}\right)\frac{P_{A1}}{P}}\right]-\frac{(X_{g1}+X_{g2})\,RT(N_A-N_B)}{D_BP}=\frac{X_mRT(N_A-N_B)}{\delta'D_BP} \tag{5}$$

where the second term allows for the presence of the external gas films and δ' corrects for the four factors.

For cases involving a continuous removal or generation of a chemical species inside porous media, steady state diffusion can also occur inside dead-end pores as well as flow pores. For diffusion-controlled reactions, dead-end and flow pore volume could be of comparable effectiveness if the dead-end pores were significant in length relative to the thickness of the porous medium. If the dead-end pore volume were equally effective as flow pore volume (the maximum possible effectiveness), one could think of the total diffusibility δ as being affected by only three of the four retarding factors [see Equation (6)].

$$\delta \leqq (\epsilon_o)\ (\tau)\ (P_s) \tag{6}$$

An equation analogous to Equation (4) would then hold for total effective diffusion coefficient and δ [see Equation (7)].

$$D_{eff} = \delta\ D_B \tag{7}$$

As a limiting case the values of D_{eff} would exceed those of D'_{eff} by the ratio of ϵ_o to ϵ_f.

Porosities

A method of measuring flow porosity based upon the penetration of pores by a liquid which wets the medium was devised to allow estimation of D_{eff}. In this measurement, the lower face of the medium is brought into contact with the surface of a liquid which has a low surface tension (to aid in wetting the medium) and a high boiling point (to minimize evaporation). The liquids used in this work were acetonyl acetone, benzyl chloride, and benzoyl chloride. The liquid rises into the pores by capillary action, displacing the air from the continuous passageways, but only partially filling the dead-ends where the pressure of trapped air opposes its entry.

After the liquid fills the continuous pores (in times ranging from a few seconds to a few minutes), the damp faces of the porous medium are rubbed with a cloth satu-

rated with the liquid to remove any excess from the surface. From the weight of the medium before and after filling and the density of the liquid, the volume of the pores filled can be calculated. Division of this value by the volume of the medium (measured by a micrometer or by mercury displacement) gives the fractional volume occupied by these pores, herein known as penetration porosity.

Liquid will penetrate the dead-end pores until the pressure of the trapped air equals the pressure exerted by the capillary action of the liquid. By assuming a contact angle of zero deg., one can find the height of rise of a liquid in an open-ended circular tube from Equation (8):

$$h = 2\gamma/\rho g r \tag{8}$$

This liquid head, minus the head of one-half of the medium thickness, determines the pressure built up in an average dead-end pore by capillary action [Equation (9)].

$$P_c = 1.97 \times 10^{-6} \frac{\gamma}{r} - 4.83 \times 10^{-4} X_m \rho \tag{9}$$

The fractional volume of dead-end pore not filled (V_1/V_o) is calculated with Equation (10), which expresses the fractional isothermal compression of the trapped gas by the liquid used for the porosity measurement.

$$V_1/V_o = 1/(1 + P_c) \tag{10}$$

The fraction which is filled (α_i) can be calculated from Equation (11).

$$\alpha_i = 1 - V_1/V_o = P_c/(1 + P_c) \tag{11}$$

Since values of α_i vary with pore radius, values are obtained for the different radii present in a medium with Equation (12), and these are weighted according to the fraction of the pore volume having these radii and summed in order to calculate α for the medium.

$$\alpha = \sum_{i=1}^{n} \alpha_i v_i \tag{12}$$

The volume fractions are obtained by integrating a curve of pore volume vs. radius as determined by porosimeter. For media containing few pores smaller than 10μ in radius, little error is introduced by using only the average pore radius in calculating α.

Since the liquid fills the flow pores and a calculable fraction of the dead-end pores in penetration porosity measurements as shown in Equation (13)

$$\epsilon_p = \epsilon_f + \alpha\epsilon_d \tag{13}$$

and the open porosity is the sum of the flow and dead-end porosities [see Equation (14)]

$$\epsilon_o = \epsilon_f + \epsilon_d \tag{14}$$

one can combine Equations (13) and (14) to eliminate ϵ_d, and express ϵ_f in terms of measurable and calculable quantities with Equation (15).

$$\epsilon_f = \frac{\epsilon_p - \alpha\epsilon_o}{1 - \alpha} \tag{15}$$

A theoretical discussion of the rise of wetting liquids into idealized dead-end capillaries is given elsewhere (13).

MATERIALS AND EQUIPMENT

Porous Media

The designation, material, dimensions, and source of the porous media used are listed in Table 1. Diffusion, electrical conductivity, porosimeter (14), and porosity measurements were made on most of these. The pore diameters of the media

TABLE 1. DESIGNATION, MATERIALS, DIMENSIONS, AND SOURCES OF POROUS MEDIA USED

Designation	Material	Dimensions	Source
CUF	Sintered Pyrex glass, ultrafine grade	60 mm. diam., 6 mm. thick	Corning Glass Works, Corning, New York
CF-3	Sintered Pyrex glass, fine grade	60 mm. diam., 3 mm. thick	Corning Glass Works, Corning, New York
CF-6	Sintered Pyrex glass, fine grade	60 mm. diam., 6 mm. thick	Corning Glass Works, Corning, New York
CF-12	Sintered Pyrex glass, fine grade	60 mm. diam., 12 mm. thick	Corning Glass Works, Corning, New York
CM	Sintered Pyrex glass, medium grade	60 mm. diam., 6 mm. thick	Corning Glass Works, Corning, New York
RA-98	Alundum	60 mm. diam., 6 mm. thick	Norton Co., Worcester, Mass.
RA-225	Alundum	60 mm. diam., 6 mm. thick	Norton Co., Worcester, Mass.
P-010	Porous porcelain	60 mm. diam., thicknesses vary from 3 to 13 mm.	Selas Corp. of America, Philadelphia, Pa.
P-015-6	Porous porcelain	60 mm. diam., thicknesses vary from 3 to 13 mm.	Selas Corp. of America, Philadelphia, Pa.
P-015-12	Porous porcelain	60 mm. diam., thicknesses vary from 3 to 13 mm.	Selas Corp. of America, Philadelphia, Pa.
P-020	Porous porcelain	60 mm. diam., thicknesses vary from 3 to 13 mm.	Selas Corp. of America, Philadelphia, Pa.
P-030	Porous porcelain	60 mm. diam., thicknesses vary from 3 to 13 mm.	Selas Corp. of America, Philadelphia, Pa.
P-040	Porous porcelain	60 mm. diam., thicknesses vary from 3 to 13 mm.	Selas Corp. of America, Philadelphia, Pa.
P-060	Porous porcelain	60 mm. diam., thicknesses vary from 3 to 13 mm.	Selas Corp. of America, Philadelphia, Pa.
A-1	Activated alumina, grade "F"	Irregular lumps roughly 25 mm. × 50 mm. × 75 mm.	Aluminum Ore Co., East St. Louis, Ill.
A-2	Activated alumina, grade "F"	Irregular lumps roughly 25 mm, × 50 mm. × 75 mm.	Aluminum Ore Co., East St. Louis, Ill.
GL	Glass beads	Spherical beads, av. diam. approx. 0.020 mm.	3M Co., St. Paul, Minn.
TiO_2	Titanium dioxide	Spherical part., av. diam. 1.3 × 10^{-4} mm.	Monsanto Research Corporation, Dayton, Ohio
BR	Sintered bronze powder, grade 46 HP	Spheroidals, —40, +60 mesh	Metals Disintegrating Co., Elizabeth, N. J.

were determined in a mercury porosimeter with pressures ranging up to 3,000 lb./sq.in. (*15, 16*). All of the pore size distributions were unimodal, except that of RA98, which was bidisperse, having maxima at both 2.5 and 13 μ.

Diffusion Apparatus

The diffusion experiments were made at steady state countercurrent conditions in an apparatus consisting of two half cells with the porous medium to be tested clamped between them. The half cells were immersed in a constant temperature bath at 30°C. during all the diffusion runs. Dry nitrogen gas (98.8% pure) was fed continuously into one half cell, and helium (99+% pure) to the other. The shape and dimensions of the cells and other apparatus used are given elsewhere (*15, 16*).

Electrical Conductivity Apparatus

Electrical conductivity measurements (*17*) were made on media impregnated with potassium chloride solutions of known strength and conductance (*18*). The media contained in a vacuum flask under pressure of less than 1 mm. Hg, were covered with the potassium chloride solution and then atmospheric pressure was restored. The liquid then filled the pores. For most of the measurements, 0.1000 N potassium chloride was used, but 0.0200 N and 0.0100 N potassium chloride were also used to check the effect of concentration.

Two pairs of opposing medium surfaces were coated with duPont Duco cement (1 to 2 mm. thick layer) prior to the conductivity measurements to prevent liquid films on the surfaces from conducting electricity.

Open porosity tests before and after coating showed that a maximum of 11.0%, but an average of only 1.7%, of the pores were filled by the cement. To correct this, the cross-sectional area of the medium in Equation (17) was multiplied by the ratio of the open porosity after coating to the open porosity before coating.

The electrical resistances of the impregnated media were measured by an impedance bridge. The two uncoated faces of the media were covered with cloth soaked in the potassium chloride solution, and were then clamped between two ⅝ in. sq. by 0.002 in. thick platinum electrodes. Short pieces of 26 gauge platinum wire were spot welded to the backs of the electrodes, which were then glued to glass backing supports. Electric leads were connected to an impedance bridge with external capacitors. The capacitors and the impedance bridge were adjusted until a minimum signal height registered on an oscilloscope, and then the resistance was recorded. One thousand cycles per second, a.c. current was used for all electrical conductivity measurements.

When the electrical conductivity of a salt-impregnated porous medium is actually measured, residual conductivity of the medium as well as the conductivity of the salt solution affects the measured resistance. To correct for this, conductivity is determined with the medium filled with distilled water. Conductivity due to the salt solution alone is then calculated by Equation (16).

$$1/R_s = 1/R_{s+m} - 1/R_m \qquad (16)$$

The net diffusibility is then calculated from Equation (17).

$$\delta' = \frac{X_m}{(\overline{C})\,(A_m)\,(R_s)} \qquad (17)$$

It is noteworthy that all the equipment needed (except the electrodes) are standard commercial items of reasonable cost which can be quickly assembled. The time required per measurement is also short, as several samples per day can be micrometered, coated, and measured by inexperienced personnel.

RESULTS

Porosities

Open and penetration porosities and porosimeter measurements were run on the same materials to allow calculation of the flow porosity. The open porosity, the penetration porosity, the liquid used in determining it, and the flow porosity, both as a fraction of total medium volume and as a percentage of total open porosity for each piece, are shown in Table 2.*

TABLE 2. POROSITIES OF POROUS MEDIA

Material	Sample No.	Open porosity	Penetration porosity	Liquid used*	α	Flow porosity	Flow porosity as a percentage of open porosity
P-060	1	0.175	0.146	BOC	0.743	0.062	35
	2	0.170	0.141	BOC	0.743	0.058	34
P-010	1	0.661	0.354	AA	0.168	0.292	44
	1	0.661	0.360	BOC	0.188	0.289	44
	1	0.661	0.374	BC	0.178	0.311	47
	2	0.661	0.389	BOC	0.188	0.324	49
	2	0.661	0.390	BC	0.178	0.330	50
P-030	1	0.413	0.360	BOC	0.500	0.308	75
	2	0.413	0.363	BOC	0.500	0.314	76
	3	0.399	0.344	AA	0.466	0.296	74
	3	0.399	0.351	BOC	0.500	0.304	76
	4	0.401	0.350	AA	0.466	0.305	76
	5	0.399	0.349	AA	0.466	0.305	76
CF-3	3	0.312	0.268	BOC	0.272	0.252	81
	4	0.322	0.282	BOC	0.272	0.267	83
	5	0.314	0.276	BOC	0.272	0.261	83
TiO_2	1	0.498	0.496	AA		0.496†	100
	2	0.500	0.500	AA		0.500†	100
	3	0.500	0.500	AA		0.500†	100
BR	4	0.392	0.389	AA		0.389†	99
	5	0.418	0.420	AA		0.420†	100
	6	0.408	0.402	AA		0.402†	98

* AA = acetonyl acetone, surface tension = 37.2 dynes/cm., density = 0.974 g./ml. BC = benzyl chloride, surface tension = 40.2 dynes/cm., density = 1.102 g./ml. BOC = benzoyl chloride, surface tension = 42.7 dynes/cm., density = 1.215 g./ml.

† Flow porosity equals penetration porosity for cases where penetration porosity equals open porosity [see Equation (15)].

The penetration porosity was determined on several pieces by different liquids on successive runs. The agreement between determinations run with different liquids indicates that this measurement is not dependent on the liquid used, but is a property of the porous medium.

Two of the samples, types TiO_2 and BR, were fabricated so as to contain essentially no dead-end pores, so that penetration and open porosities could be compared for cases where they should be equal. The 1.9 cm. diameter × 1.0 cm. high cylindrical TiO_2 samples were formed by mixing the powder with less than 0.1% polyvinyl acetate binder and then by cold pressing at 4,500 lb./sq.in. The 1.2 cm. diameter × 1.0 cm. high cylindrical BR samples were formed by sintering the powder in a mold for 15 min. at 840°C. under dissociated ammonia. Data in Table 2 show that the penetration and open porosities are indeed equal within experimental error for both of these loosely consolidated materials. This shows that liquids theoretically capable of filling all of the flow pores actually do this quantitatively.

Net Diffusibilities

Values of net diffusibility were calculated from diffusion data (*15, 16*) with Equation (5) and are recorded

* Additional data have been deposited as document 8680 with the American Documentation Institute, Photoduplication Service, Library of Congress, Washington 25, D. C., and may be obtained for $1.25 for photoprints or 35-mm. microfilm.

TABLE 3. NET DIFFUSIBILITIES

Material	Mean pore radius, μ	Average net diffusibility from diffusion measurements	Average net diffusibility from electrical conductivity measurements
CF-3	2.21	0.159	0.176
CF-6	2.21	0.167	0.177
CF-12	2.21	0.167	0.201
CM	3.96	0.159	0.174
RA-98	7.47	0.0908	0.0908
RA-225	11.1	0.0962	0.0932
P-015-6	0.94	0.220	0.246
P-015-12	0.94	0.203	0.170
P-020	0.76	0.166	0.167
A-1	13.7*	0.113	0.080
A-2	3.98*	0.0594	0.0514
GL	6.42*	0.294	0.281
CUF	0.49	0.0598	0.0846
P-030	0.62	0.151	0.188
P-040	0.42	0.114	0.147
P-060	0.26	0.0385	0.0494

* Pore radius from flow measurements.

in Table 3. The average standard deviation of these measurements was 3.4%.* Values of net diffusibility calculated from electrical conductivity measurements with Equations (16) and (17) are also recorded in Table 3. Standard deviation of these measurements was 5.2%.*

A plot of net diffusibility from diffusion vs. net diffusibility from electrical conductivity measurements for media CF, CM, RA-98, RA-225, P-015, P-020, A-1, A-2, and GL is shown in Figure 1. The slope of this graph forced through the origin is 0.98, with 0.90 and 1.06 as 95% confidence limits. Media CUF, P-030, P-040, and P-060 were excluded from this correlation, because they contained large fractions of pores smaller than ten times the mean free path.

* See footnote on page 324.

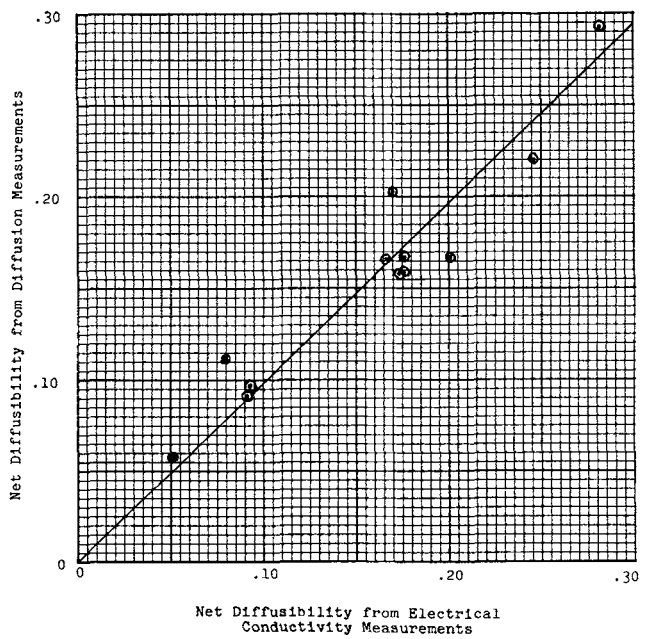

Fig. 1. Graph of net diffusibility from diffusion measurements vs. net diffusibility from electrical conductivity measurements.

DISCUSSION

Porosities

The open and penetration porosities were the same for the BR and TiO_2 pellets, which should not contain any dead-end pores. This shows that the penetration porosity measurement does fill all the flow pores, as was assumed in the derivation of the formula for calculation of the flow porosity.

All the other media tested, except the beds of glass beads, were more strongly consolidated than the BR and TiO_2 pellets, and it seems probable that they had been strongly sintered while being fabricated. One would expect that this sintering would produce a considerable number of dead-end pores, as indicated by the penetration porosity measurements. In all these cases, both ϵ_p and ϵ_f were significantly less than ϵ_o.

The values of ϵ_p are reproducible for a given sample, which tends to indicate that a fundamental property of the material is being measured. The dispersions in the measurements of ϵ_p and ϵ_o are similar for both types of determinations, and a large fraction, if not all, of the variation in both cases can be attributed to nonreproducibility in wiping the excess liquid off the sides of the media.

The values of ϵ_f seem to be independent of the liquid used in measuring it, providing it wets the medium. When attempts were made to perform ϵ_p measurements with water and ethylene glycol, the media surfaces were wetted in some spots but not in others, and the weights of liquid absorbed were irregular. However from Table 2 we note that the calculated values of ϵ_f agree closely when liquids having low surface tension, such as acetonyl acetone, benzyl chloride, or benzoyl chloride, are used.

The values of pore radius used to calculate ϵ_f were read off porosimeter curves of pore volume vs. pore radius. In a porosimeter measurement, the mercury, upon reaching a constriction in a pore, remains there until the pressure is raised enough to force the mercury through; then it fills the volume behind the constriction up to the next smaller constriction, but this intervening volume is interpreted as being composed of pores having the diameter of the first constriction. On the other hand, acetonyl acetone or other wetting liquid under capillary pressure would penetrate up to a limiting enlargement. The use of pore radius from porosimeter measurements in calculating ϵ_f, therefore, assumes that the dead-end pores have the same average pore shape and size distribution of constrictions and enlargements as the total collection of pores. This assumption is not a serious limitation, however. The values of flow porosity calculated are rather insensitive to the values of pore radius used, unless the medium contains a large fraction of pore volume with radius smaller than 1μ and has a penetration porosity considerably smaller than its open porosity.

Pores with diameters smaller than 0.1μ are almost completely filled by penetration porosity measurements at atmospheric pressure; hence, this method, as outlined above, is able to distinguish between flow and dead-end pores only in media containing enlargements larger than this. Adaptation of this measurement to higher pressure might enable this limit to be lowered.

Tortuosity, Pore Shape Factor

Assuming a value of 1/1.41 for tortuosity (2), one can calculate pore shape factors by using the δ' and ϵ_f data in Equation (3). The range of pore shape factors was 0.40 for RA-225 to 1.20 for P-020. This impossible result for P-020 indicates that the pores have a preferred orientation in this material, and the tortuosity cannot be assumed to have a constant value in all cases. The values

of 0.98, 0.96, and 0.95 for CF-6, P-015-12, and P-015-6 are also suspiciously high.

Net Diffusibilities

An accuracy of ± 10% is postulated for the net diffusibility values from diffusion measurements, based on the dispersion of the data and an estimate of the error in the diffusion measurements.

The values of net diffusibility from electrical conductivity measurements recorded in Table 3 have approximately the same dispersion as those from diffusion data. Because the diffusion disks were fairly large, and it was necessary to cut them into pieces before making the electrical conductivity measurement, some randomness from sampling is to be expected. Due to cutting losses and to the circular edges of the disks, which could not be cut into cubes, no more than one-third of any disk was actually used in the electrical conductivity measurements. In the cases of the two alumina samples and the glass beads, the original diffusion samples could not be found, so similar samples of the same materials were used. The net diffusibilities calculated from the electrical conductivity measurements using the three different solution concentrations were essentially the same.

For the media used in this work, the change from bulk diffusion to a mixture of bulk and Knudsen diffusion seems to occur when a significant fraction ($> 1/4$) of the pores have radii approximately five times the mean free path rather than ten times as suggested by Wheeler (2). The mean free path of equimolar nitrogen-helium mixtures at 740 mm. Hg and 30°C. was calculated to be 0.15μ, with Equation (18).

$$\lambda = \frac{0.707}{\pi(\sigma_{AV})^2 C_T} \tag{18}$$

Table 4 lists pores radius distribution data for media P-015 and P-020 for which δ' from diffusion and electrical conductivity measurements agreed and for media CUF, P-030, P-040, and P-060 where they deviated.

It is apparent that the presence of a large fraction of pore volume with radii smaller than 1.0μ does not necessarily cause disagreement between δ' measured by the two different methods for P-015 and P-020. However, δ' for media CUF, P-040, and P-060, composed almost entirely of pores smaller than 0.6μ and of P-030 with a large fraction of pores smaller than 0.8μ in radius, did not agree closely when measured by the two different methods. For these last four media, δ' from diffusion measurements was lower than the values obtained from electrical conductivity measurements, which is consistent with the supposition that the slower, mixed bulk-Knudsen diffusion was occurring. Since electrical conductivity measurements are a reliable measure of δ' only for macroporous media, diffusion measurements must be used for media containing micropores or pores in which mixed diffusion is expected.

Table 4. Pore Radius Distributions

Medium	Volume percent of open pore volume with radii <0.6μ	<0.8μ	<1.0μ
δ' elec. cond. = δ' diff. meas.			
P-015	3	19	66
P-020	4	19	69
δ' Elec. cond. > δ' diff. meas.			
CUF	86	99	100
P-030	1	37	87
P-040	99	100	100
P-060	93	96	99

The average length of dead-end pores, which is probably similar in magnitude to the average distance between intersections of pores, is of importance in deciding whether dead-end pores contribute significantly to diffusion inside porous media. A method of estimating this average length, based on porosity and pore radius measurements, is suggested below. For an average pore diameter of d_i cm., the cross-sectional area would be $\pi/4\ (d_i)^2$ sq.cm. The length of pores of various diameters per cc. of medium can be estimated with Equation (19).

$$l_i = \frac{f\epsilon_o}{\frac{\pi}{4}(d_i)^2} \tag{19}$$

Assuming the media are isotropic, one can consider one-third of this length to be running in each of the three dimensions. Pores entering one face of the cube would have a chance of intersecting the longitudinal cross-sectional area of the pores running in the other two directions. For penetration of 1μ

$$A_i = \frac{2}{3}(l_i \times d_i \times 10^{-4}) = \frac{8f\epsilon_o \times 10^{-4}}{3\pi\ d_i} \tag{20}$$

This area would equal the probability of a pore intersecting a pore diameter d_i as it traversed the 1μ thickness of the medium, and the summation of A_i over all d_i would equal the probability of intersecting any pore. The reciprocal of the summation would be the estimated pore length between intersections. In most cases, the equation for estimated pore length between intersections can be simplified with little error to Equation (21).

$$\overline{l} = \frac{3\pi\overline{d}}{8\epsilon_o\ (10^{-4})} \tag{21}$$

Whether or not the diffusibility is affected by dead-end pores depends both on their length and on the distribution of pore diameters within a porous medium. Dead-end pore volume connecting with the surface of the medium should be as effective as flow pore volume equidistant from the surface; however, the volume of these dead-end pores will usually be negligible. Dead-end pores, which are short relative to pellet diameter, are probably ineffective in contributing to diffusion in all cases, and Equations (3) and (4) should be used in these cases. However, in the case of dead-end pores which are significant in length compared to pellet diameter, these pores could become important. Consider the case of a porous medium containing large diameter flow pores which are joined by a much larger number of smaller diameter flow and dead-end pores. The smaller diameter pores contain most of the reacting surface area and would contain a large fraction of the resistance to diffusion. Since the porosimeter measurements have shown a wide range of pore sizes for all media measured in these experiments, it is quite possible for media to have large flow pores with ten times the diameter and one hundred times the cross-sectional area as smaller flow and dead-end pores.

In cases with a relatively large diffusion resistance in the smaller diameter pores, the dead-end porosity could tend to contribute to the effective diffusion, and Equations (6) and (7) would serve as upper estimates of the total effective diffusion coefficient.

For a medium such as A-1 with $\epsilon_o = 0.268$, $\epsilon_f = 0.157$, and $\overline{d} = 27.4\mu$, the estimated distance between intersections of pores would be 120μ, which is significant compared with the 1,590μ radius of a 1/8-in. diameter spherical pellet. The average estimated distance between pore intersections for thirteen other media was calculated to be 20μ, with a range from 3 to 45 μ. Diffusion in dead-end

pores can certainly be neglected at the lower end of this range.

It should be noted that net diffusibility is really a shape factor, and the four factors of which it is composed (ϵ_o, ϵ_f/ϵ_o, Υ, and P_s) should not be affected by temperature or pressure changes. It should be independent of temperature, pressure, or particle size and hence need not be measured at reaction conditions. Since the electrical conductivity measurements are difficult to make on irregular pieces or on pieces smaller than ⅛ in. × ⅛ in. in cross section, one could make these and the porosity measurements on larger pieces of a material to be tested and then grind or cut them up to the desired size before measuring the particle size and the reaction rate.

CONCLUSIONS

One could conclude from this work that the penetration porosity method described in this paper does measure flow porosity, since it yields reasonable values which are reproducible, is independent of the liquid used as long as it wets the medium, and has been shown to be correct for media containing no dead-ends. It has been verified that net diffusibility, which corrects the bulk diffusion coefficient for the four retarding effects present in porous media, can be successfully predicted by means of electrical conductivity measurements as long as at least 75% of the pore volume has radii greater than five mean free paths. It is pointed out that relatively long dead-end pores could be effective in contributing to diffusion inside porous media and a means of estimating their lengths is described.

NOTATION

A_i = cross-sectional area of pores split lengthwise in a 1 cm. × 1 cm. × 1μ volume, sq.cm.
A_m = cross-sectional area of porous medium, sq.cm.
c_{av} = average molecular diameter, cm.
$\overline{C}$ = specific conductivity of salt solution, mho/cm.
C_T = total concentration, molecules/cc.
$\overline{d}$ = average pore diameter, cm.
D_B = diffusion coefficient in free space, sq.cm./sec.
D_{eff} = total effective diffusion coefficient inside porous medium, sq.cm./sec.
D'_{eff} = net effective diffusion coefficient inside porous medium, sq.cm./sec.
d_i = pore diameter, cm.
D_p = diameter of a sphere having the same external area as the actual external area of the catalyst particle, cm.
E_A = effectiveness factor, dimensionless
f = fraction of open porosity having an average diameter of d_i, dimensionless
g = acceleration of gravity, cm./sec.^{2}
h = height of capillary rise into a pore, cm.
k = first-order reaction rate constant, cc. of reactant gas at reaction temperature and pressure per cc. of catalyst particles per sec.
$\overline{l}$ = estimated distance between pore intersections, μ
l_i = length of pores of diameter d_i per cc. of medium, cm.
m_T = Thiele modulus, dimensionless
N_A, N_B = diffusion fluxes, g.-moles of gases A and B diffusing per sq.cm. per sec.
P = total pressure on system, atm.
P_{A1}, P_{A2} = partial pressure of gas A at points 1 and 2, atm.
P_c = pressure generated by capillary action, atm.
P_s = pore shape factor, dimensionless
r = pore radius, cm.
R = perfect gas law constant, (cc.)(atm.)/(g.-mole)(°K.)
R_m = residual resistance of porous medium filled with distilled water, ohms
R_{s+m} = resistance of porous medium and salt solution in pores, ohms
R_s = resistance of salt solution, ohms
T = absolute temperature, °K.
V_o = volume of dead-end pore before penetration porosity measurement, cc.
V_1 = volume of dead-end pore unfilled during penetration porosity measurement, cc.
v_i = fraction of pore volume having a given average radius, dimensionless
X = distance between points 1 and 2, cm.
X_{g1}, X_{g2} = thickness of gas films, cm.
X_m = thickness of porous medium, cm.

Greek Letters

α = fraction of all dead-end pores filled during a penetration porosity measurement, dimensionless
α_i = fraction of dead-end pore of a given radius filled during a penetration porosity measurement, dimensionless
γ = surface tension of liquid, dynes/cm.
δ = total diffusibility, dimensionless
δ' = net diffusibility, dimensionless
ϵ_d = fraction of porous medium volume occupied by dead-end pores, dimensionless
ϵ_f = fraction of porous medium volume occupied by flow pores, dimensionless
ϵ_o = open porosity, dimensionless
ϵ_p = penetration porosity, dimensionless
λ = mean free path of gas molecules, cm.
ρ = density, g./cc.
Υ = tortuosity, dimensionless

LITERATURE CITED

1. Hoogschagen, J., *Ind. Eng. Chem.*, **47**, 906 (1955).
2. Wheeler, A., in "Advances in Catalysis and Related Subjects," W. G. Frankenberg, V. I. Komarewsky, and E. K. Rideal, ed., Vol. III, pp. 249-327, Academic Press, New York (1951).
3. Wagner, C., *Z. Phys. Chem.*, **A193**, 1 (1943).
4. Goodknight, R. C., and I. Fatt, *J. Phys. Chem.*, **65**, 1709 (1961).
5. Stewart, C. R., A. Lubinski, and K. A. Blenkarn, *J. Petrol. Tech.*, **13**, 383 (1961).
6. Schofield, R. K., and C. Dakshinamurti, *Disc. Faraday Soc.*, **3**, 56 (1948).
7. Klinkenberg, L. J., *Bull. Geol. Soc. Am.*, **62**, 559 (1951).
8. Scott, D. S., and K. E. Cox, *J. Chim. Phys.*, **57**, 1010 (1960).
9. Arnold, H. J., *Ind. Eng. Chem.*, **22**, 1091 (1930).
10. Gilliland, E. R., *ibid.*, **26**, 681 (1934).
11. Hirschfelder, J. O., C. F. Curtiss, and R. B. Bird, "The Molecular Theory of Gases and Liquids," pp. 578-582, Wiley, New York (1954).
12. Sherwood, T. K., and R. L. Pigford, "Absorption and Extraction," p. 5, McGraw-Hill, New York (1952).
13. Altshuler, M. A., *Colloid J.*, **23**, 543 (1961).
14. Ritter, H. L., and L. C. Drake, *Ind. Eng. Chem. Anal. Ed.*, **17**, 782 (1945).
15. Lavacot, F. J., D.Sc. dissertation, Washington Univ., St. Louis, Mo. (1952).
16. Wang, S. L., D.Sc. dissertation, Washington Univ., St. Louis, Mo. (1953).
17. Hedley, W. H., D.Sc. dissertation, Washington Univ., St. Louis, Mo. (1957).
18. Hodgman, C. D., "Handbook of Chemistry and Physics," 33 ed., p. 2149, Chemical Rubber Publishing Co., Cleveland, Ohio (1952).

Manuscript received January 21, 1965; revision received October 8, 1965; paper accepted October 11, 1965.